Journal of Catalysis 286 (2012) 260–265

Contents lists available at SciVerse ScienceDirect

Journal of Catalysis

journal homepage: www.elsevier.com/locate/jcat

Understanding the spatial distribution of coke deposition within bimodal micro-/mesoporous catalysts using a novel sorption method in combination with pulsed-gradient spin-echo NMR

Li Min Chua [a,b], Iain Hitchcock [a], Robin S. Fletcher [b], Elizabeth M. Holt [b], John Lowe [c], Sean P. Rigby [d,*]

[a] Department of Chemical Engineering, University of Bath, Claverton Down, Bath BA2 7AY, UK
[b] Johnson Matthey Technology Centre, P.O. Box 1, Belasis Avenue, Billingham, Cleveland TS23 1LB, UK
[c] Department of Chemistry, University of Bath, Claverton Down, Bath BA2 7AY, UK
[d] Department of Chemical and Environmental Engineering, University of Nottingham, University Park, Nottingham NG7 2RD, UK

ARTICLE INFO

Article history:
Received 8 September 2011
Revised 4 November 2011
Accepted 17 November 2011
Available online 22 December 2011

Keywords:
Zeolite
Chemisorption
Coke
Deactivation
Pore network
Diffusion
NMR
Nonane
Adsorption

ABSTRACT

A new method for the determination of the spatial distribution of metal surface area within bimodal micro-/mesoporous solids has been developed. This novel technique involves incorporating a nonane pre-adsorption stage between two successive chemisorption experiments. This method has been used to probe the distribution of platinum amongst the micropores and mesopores of a range of bi-functional PtH-MFI catalysts, each possessing differing surface acidities, which have been used for benzene alkylation with ethane. It has been found that the catalyst with the lowest Si/Al ratio, and thus highest number of acid sites, also possessed the largest metal surface area within its microporosity. This catalyst was also the one that deactivated most rapidly, with coke being deposited predominantly within the micropore network. This was attributed to the bi-functional mechanism for coke formation at higher temperatures. Pulsed-gradient spin-echo NMR has also been used to show that a combination of higher mesopore platinum concentration and higher mass transport rates facilitated greater coke deposition within the mesoporosity.

1. Introduction

Alkylation of benzene with ethene is currently used to synthesise ethylbenzene, a vital intermediate in the manufacture of polystyrene. However, the process is very energy intensive, involving naphtha reforming. A potential alternative is the direct alkylation of benzene with ethane using a bi-functional catalyst that performs both the dehydrogenation and alkylation steps. Platinum on MFI zeolite has been proposed as a potential catalyst, and the reaction studied in detail [1]. However, under certain conditions, the catalyst deactivates rapidly by coking. In order to better design the process, a detailed understanding of the coking mechanisms is essential. In previous work [1], it was shown that zeolites with differing Si/Al ratios gave rise to differing coking behaviour. In particular, it was found that coke was predominantly deposited in different locations, depending on the Si/Al ratio, with more losses of surface area due to coke arising within the microporosity at lower values of the ratio, and in the mesopore network at higher values. In this work, the reasons for the particular coke distribution in different catalysts will be explored. In particular, it will be shown that the spatial distribution of platinum and the mass transfer rates contribute to the coke location. To facilitate this study, a novel method for determining the spatial distribution of platinum within the catalyst has been developed based upon the nonane pre-adsorption method, previously used to assess microporosity [2].

Methods for studying the spatial distribution of platinum nanoparticles within heterogeneous catalysts have been developed but have their limitations. The spatial arrangement of platinum nanoparticles has been observed directly using electron tomography [3]. However, the characteristic overall dimension of the sample volume that can be studied is only ~500 nm, and thus these data may be statistically unrepresentative of a real macroscopic catalyst pellet. Pressure-jump IR spectroscopy of adsorbed CO has been used to study spatial locations of platinum particles but can only distinguish internal from external particles [4]. Hence, there is a lack of a technique that can provide more representative information on the location of platinum nanoparticles within a bimodal micro-/mesoporous system.

The balance between mass transport and reaction rates is known to influence the pattern of coke lay-down in catalysts, and thus has been the subject of extensive modelling work [5].

* Corresponding author.
E-mail address: enzspr@exmail.nottingham.ac.uk (S.P. Rigby).

0021-9517/$ - see front matter © 2011 Elsevier Inc. All rights reserved.
doi:10.1016/j.jcat.2011.11.012

Coke distribution and mass transport in catalyst pellets deactivated by coke deposition have been studied previously using a range of NMR methods. Cheah et al. [6] used MRI methods to study the spatial distribution of coke within catalyst pellets over macroscopic dimensions. While these studies revealed the heterogeneous spatial distribution of coke deposits, due to the variation in relaxation time of the static imbibed fluid over fresh and coked surfaces, only qualitative information could be obtained. Stapf et al. [7] probed the spatial distribution of coke residues in porous catalyst pellets using field-cycling relaxometry. Pulsed-gradient spin-echo (PGSE) (also known as pulsed-field gradient (PFG)) NMR has been used [8,9] to determine how the tortuosity of a porous catalyst pellet varies with coking levels. In this work, PGSE NMR will be used to measure mass transport rates in the mesopore network of the bimodal PtH-MFI catalysts.

This paper is constructed as follow. First, a theory, concerning how both the spatial arrangement of platinum metal and mass transport rates can effect coking, will be outlined. Then, the new method to obtain an experimental measurement of the spatial distribution of platinum metal will be described. It will then be seen how data obtained from this new method can shed light on the reasons for the different distributions of coke deposition for different catalysts observed in earlier work.

2. Theory

2.1. Pulsed-gradient spin-echo (PGSE) NMR

For more details on the PGSE (or PFG) NMR method, the reader is referred to earlier work by Hollewand and Gladden [10]. In PFG-NMR, the echo attenuation, R, is defined as the ratio of the echo intensity in the presence of a gradient ($M(g)$) to the echo intensity in the absence of a gradient ($M(0)$). For the NMR pulse sequence (detailed below) used in this work, the echo intensity variation for a single component diffusion is given by:

$$R = \frac{M(g)}{M(0)} = \exp\left[-D\gamma^2 g^2 \delta^2 \left(\Delta - \frac{\delta}{3} - \frac{\tau}{2}\right)\right], \quad (1)$$

where D is the diffusion coefficient, γ is the gyromagnetic ratio, g is the pulsed-field gradient strength, δ is the duration of the pulsed gradient, Δ is the diffusion time and τ is the correction time between bipolar gradients. A range of echo attenuations are obtained by varying g, and a plot of $\ln R$ against $\gamma^2\delta^2 g^2(\Delta - \delta/3 - \tau/2)$ yields the diffusion coefficient from the slope of the straight line fit to the data. Since the observed signal contains a contribution from the spin density, which is directly related to voidage, the diffusion coefficient measured by PFG-NMR, D_{PFG} is given by [10]:

$$D_{PFG} = \frac{D_w}{\tau_p}, \quad (2)$$

where D_w is the free diffusion coefficient for bulk liquid at the temperature that the PFG-NMR experiment is conducted at, and τ_p is the tortuosity of the pore space occupied by the fluid. However, given that differences in chemistry and molecular size/shape may mean different liquids have varying levels of interaction with a given type of pore wall surface, which may affect transport along the pore to differing extents, the tortuosities obtained are particular to a specific liquid-adsorbent combination. For more complex systems, the expression for the PFG-NMR log-attenuation will be different to that shown in Eq. (1). In heterogeneous systems, where different regions of the sample do not (significantly) exchange molecules during the course of the PFG-NMR experiment, but have different diffusivities, the NMR signal would be a composite of a set of expressions similar to Eq. (1), weighted by the volume fraction of each region.

2.2. Coking model

Guisnet and Magnoux [11] suggested that, for bifunctional metal/acid catalysis at high reaction temperatures, the coking process occurs by a bi-functional mechanism involving various steps that occur over acid and metallic sites, and that the coke deposits formed are polyaromatic. In our earlier work concerning benzene alkylation with ethane over a PtH-MFI catalyst at 370 °C [1], IR spectra of the coke deposits indicated the presence of polyaromatic species, which suggested that hydrogen transfer (acid catalysts) and dehydrogenation steps (bifunctional catalysts) took place during the coking reaction. A bifunctional mechanism would necessitate coke precursor molecules moving between acid and metal sites. Hence, in a mesoporous environment, where molecules could potentially escape the catalyst surface for the bulk void space of the pore, it might be anticipated that the overall rate of the coking reaction would be proportional to the rate at which coke precursor molecules could move from one type of site to another, and also the spatial concentration of each type of site. Hence, if the diffusivity of molecules and the concentration of metallic sites could be measured, then it would be expected that the overall rate of coking, and hence some measure of amount of coke build up over a given period of time, would be proportional to the product of the diffusivity and metal site concentration. However, within the confinement of micropores, the metal and acid sites would be in very close proximity, and there would be no opportunity for the adsorbed molecules to escape directly into the gas phase and bypass surface sites. Hence, the reaction rate might then be expected to be proportional to the capacity of available sites. Since it is expected that the acid sites would be pervasive across the zeolite surface, then, overall, the metal sites might then be expected to be the rarer, and thus rate-controlling.

3. Experimental

3.1. Materials

The materials studied in this work were two 1 wt.% Platinum-MFI (ZSM-5) catalysts prepared from parent zeolites with Si:Al ratios of 15 and 40 (denoted Pt H-MFI-15 and Pt H-MFI-40, respectively), as described in earlier work [1]. The coked samples were obtained following catalyst use for benzene alkylation with ethane carried out at atmospheric pressure in a continuous flow reactor at 370 °C, as described in earlier work [1]. The amount of coke formed on the used catalysts at different TOS is summarised in Table 1. In spite of an increase in the coke content, the rate of coke deposition declined with time after a rapid increase in the amount of carbonaceous deposits at 4 h TOS.

In earlier work [1], the BET surface areas for the fresh and coked Pt H-MFI-15 and Pt H-MFI-40 catalysts were obtained using both nitrogen and argon, adsorption, and are shown in Table 2. The surface area decreased with TOS, indicating that parts of the zeolite pore network were blocked or isolated by coke molecules formed. Further, in previous work [1], the pore size distributions (PSD) of the PtH-MFI catalysts were obtained, using the Horvath–Kawazoe

Table 1
Values of coke content on coked PtH-MFI catalysts after different time-on-stream (TOS). The coke content measured has a standard error of ±0.03%.

Time-on-stream (h)	Total coke (mass%)	
	PtH-ZSM-5(30)	PtH-ZSM-5(80)
4	1.83	0.76
24	3.39	–
48	5.61	2.00

Table 2
BET surface area for Pt-zeolite catalysts at different TOS.

Time-on-stream (TOS) (h)	BET surface area ($m^2 g^{-1}$)			
	PtH-ZSM-5(30)		PtH-ZSM-5(80)	
	Nitrogen	Argon	Nitrogen	Argon
0	369.1	389.7	428.6	444.6
4	347.8	347.2	384.8	398.1
24	322.1	321.5	–	–
48	282.2	277.8	339.6	383.9

cylindrical pore model [12], from the nitrogen adsorption data. For example, for the Pt H-MFI-15 catalyst, the differential pore volume plot of the fresh catalyst showed three peaks at 0.725 nm, 0.743 nm and 0.749 nm. As the carbon content increased, the intensity of the three peaks progressively decreased, and the PSD was shifted towards smaller pore diameters. A significant apparent increase in the micropore volume was observed at a pore diameter of 0.72 nm for the 4 h coked catalyst and 0.71 nm for the 24 h coked catalyst.

3.2. Determination of spatial distribution of metal

This study has used a nonane pre-adsorption method to determine the location of platinum in PtH-MFI catalysts and is explained as follows using the schematic depictions shown in Fig. 1. At Stage 1, the metal surface area was determined using carbon monoxide chemisorption. The carbon monoxide was able to access the platinum in the micropores, the mesopores and the outer surface of the zeolite crystallites. Following this, the sample was then exposed to a saturated atmosphere of nonane, which filled the micropores and mesopores with adsorbed nonane (Stage 2). The sample was then evacuated at 70 °C, thereby leaving the nonane remaining only in the micropores (Stage 3). This is because nonane has a high physisorption energy and, thus, it can only be removed from the micropores at high temperatures (~400 °C) and vacuum [12]. Following evacuation, a second carbon monoxide chemisorption experiment was then carried out, but the carbon monoxide was then no longer able to access the platinum in the micropores (Stage 4). This is because the sizes of pores in ZSM-5 are 5.4 × 5.6 Å [13]. Rouquerol et al. [14] report that the width of a *n*-nonane molecule is 4 Å, and Roszak and Balasubramanian [15] report the bond length of a platinum–carbon and a carbon–oxygen bond is 1.88 Å and 1.14 Å, respectively. This means that when nonane is situated in the micropores of a PtH-MFI zeolite, no carbon monoxide molecules are able to enter them and chemisorb to the platinum surface. Therefore, the calculated metal surface area following nonane pre-adsorption will be for the platinum in the mesopores and the outer surface only. This means that the total amount of metal in the micropores and the mesopores/outer surface can be calculated using the above method.

The stoichiometry of the interaction between the gas and the metal needs to be known before a metal surface area can be calculated. The stoichiometry between carbon monoxide and platinum can vary between 1 and 2 [16]. This is because carbon monoxide can either bond linearly to a platinum atom (stoichiometry is 1) or it can bridge between two platinum atoms (stoichiometry is 2). In this work, a stoichiometry factor of 1 will be used and is justified as follows. The degree of carbon monoxide bridging is governed by the acidity of the support [17]; as a support becomes less acidic, there become more bridging carbon monoxide molecules. It is thought that this is because increased basicity means the electron density on the Pt-clusters increases. This means more platinum atoms can contribute to back-bonding. Thomas et al. [18] used infra-red spectroscopy to determine whether carbon monoxide formed linear or bridging bonds to platinum in a Pt-ZSM-5 catalyst. They found that the carbon monoxide formed linear bonds to the platinum. The Si:Al ratio for their zeolite was 50, while the Si:Al ratios for the zeolites that are to be studied in this work are 40 and 15. Hence, the supports used in this study, therefore, have more acidic sites than the one used by Thomas et al. [18]. This means that it is reasonable to assume that the stoichiometry factor for carbon monoxide on platinum, in this study, will also be 1. Other

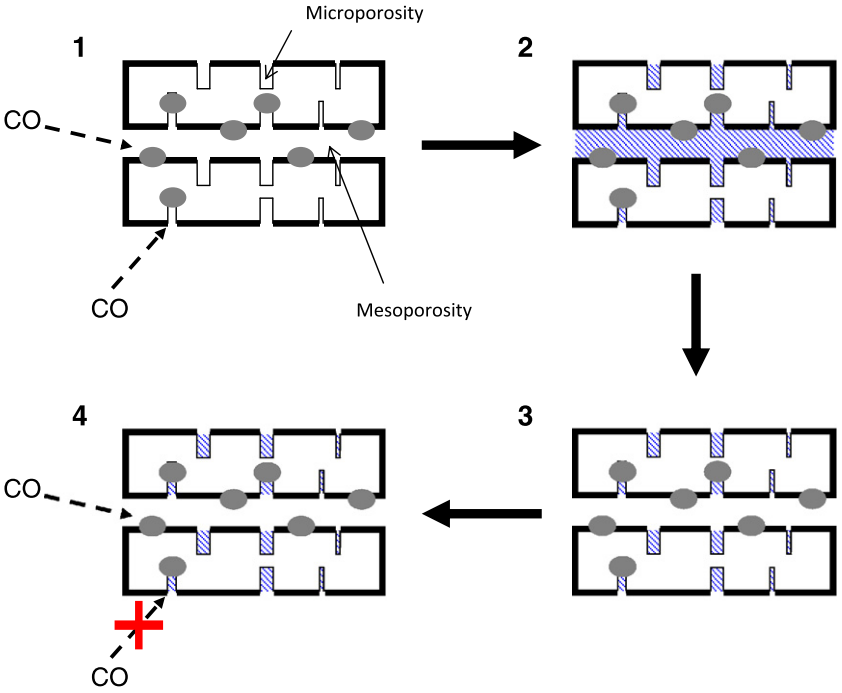

Fig. 1. Schematic diagram depicting the stages of the method to determine the spatial distribution of platinum metal within the bimodal catalyst based on MFI zeolite. The grey ovals depict platinum metal sites, while the cross-shaded regions depict adsorbed nonane.

studies have also used a stoichiometry factor of 1 when studying carbon monoxide chemisorption on a Pt-ZSM-5 catalyst [19–22].

Lepage et al. [23] have shown, using infra-red spectroscopy, that the pore curvature has little effect on the stoichiometry factor for carbon monoxide on platinum. They studied a range of different systems, including microporous, mesoporous and macroporous silicas, with a 1% platinum loading, and found the ratio between the bridging and linear bonded carbon monoxide molecules to be approximately the same. Therefore, it will be assumed in this study that the stoichiometry factor for carbon monoxide chemisorbing onto platinum in the micropores, the mesopores and the outer surface is the same.

3.2.1. Metal surface area analysis before nonane adsorption

Pt metal surface areas were measured on a Micromeretics ASAP 2010 instrument by CO chemisorption. The sample was initially evacuated at 250 °C for 4 h to remove any physisorbed gases from the surface of the catalyst. Samples evacuated for longer periods did not show any further mass loss. Reduction of the catalyst was carried out using a flow of H_2 (20 ml min^{-1}) at 70 °C for 12 h, which also removed the H_2O produced. The system was then evacuated at 70 °C for a further 12 h to remove H_2. The sample was then cooled to 35 °C, and the adsorption isotherm was measured in the pressure range 100–760 mm Hg of CO. The system was evacuated once more at 35 °C for 30 min to remove the weakly bound CO, and following this, a second isotherm was studied at 35 °C. The amount of CO adsorbed was evaluated by calculating the difference between the two isotherms and extrapolating the linear part of the difference back to zero pressure.

3.2.2. Nonane pre-adsorption

After the second isotherm, the sample was back-filled with nitrogen gas and transferred to a desiccant chamber with a beaker of liquid nonane. The sample was left for a week to absorb the nonane vapour.

3.2.3. Metal surface area analysis after nonane adsorption

Following nonane pre-adsorption, the sample was transferred back to the chemisorption apparatus and evacuated to vacuum at 70 °C for 12 h. This particular thermal treatment regime was developed as follows. Following the filling of the sample with nonane, it was thermally treated at the trial temperature for a series of successive periods of time. After each successive time period, nitrogen sorption isotherms were obtained. The heat treatment continued until the hysteresis loop region of the nitrogen isotherms for the nonane-filled sample matched that for the fresh sample, following suitable adjustment (by a constant amount) of the amount adsorbed to account for nonane still retained in the micropores. For example, Fig. 2 shows the superposed nitrogen sorption isotherms obtained for the fresh parent zeolite and the same sample following filling with nonane and then evacuation at 70 °C for 12 h. From Fig. 2, it can be seen that this particular pre-treatment regime results in a good overlap of the hysteresis loops. This finding suggested that all of the nonane had been successfully removed from the sample mesoporosity, and, thus, the remaining nonane is located only within the micropores, where it blocks access for nitrogen. The multi-layer build-up region (relative pressures <0.4) of the nitrogen adsorption isotherm for the fresh sample was fitted to a two-component Langmuir and BET isotherm model, as described in earlier work [1]. The Langmuir component of the model accounted for adsorption within the sample microporosity. It was found that the ratio of the adjustment in the amount adsorbed for the isotherms for the nonane-containing sample shown in Fig. 1, to the micropore capacity from the Langmuir component for the fresh sample, suggested that >90% of the initial micropore capacity remained occupied with nonane following evacuation at

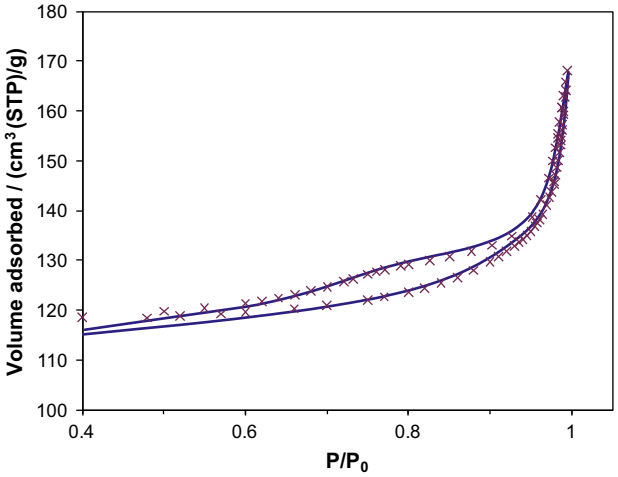

Fig. 2. Nitrogen sorption isotherms obtained (at 77 K) for the fresh parent zeolite (solid line), and for the same sample following nonane pre-adsorption and evacuation to vacuum at 70 °C for 12 h, with the amount adsorbed adjusted upwards by a constant value of 80.4 $cm^3(STP)g^{-1}$ for all data points (×).

70 °C for 12 h. The slight loss of nonane from the microporosity may be only that weakly bound within microporous ruts of the shallow surface roughness of the mesopores. Since platinum crystallite obstacles probably hinder adsorbate diffusion, the fresh sample will probably have the most rapid diffusional exchange possible. Following the evacuation regime, the experimental procedure to reduce the catalyst with H_2 and measure the CO adsorption isotherms was repeated.

3.2.4. Validation of the new method

It is conceivable that exposure of the metal surface to nonane pre-adsorption may have some effect on the assumed CO stoichiometry factor of unity. In order to test this possibility, we have compared CO metal surface areas, for a model system consisting of a solely mesoporous, 0.6 wt.% Pt on Al_2O_3 catalyst, obtained before and after filling of the mesoporosity with nonane. A solely mesoporous model system was chosen because, in the Pt-zeolite catalyst samples studied in this work, it is only the metal surface area located within the mesoporosity that is re-measured, following exposure to nonane. It was found that the nonane adsorption and subsequent removal processes made no statistically significant difference to the metal surface area of the Pt-alumina catalyst, as measured by CO chemisorption.

3.3. PFG-NMR

Prior to exposing the catalyst to the hydrocarbon liquids, the zeolite catalysts were first heated up to 250 °C under vacuum for 4 h to remove any physisorbed species. Then, the, initially dry, solid was suspended above a reservoir of liquid hydrocarbon in a sealed vessel, and the system left, for at least 24 h, to allow it to achieve equilibrium, in a water bath set at 25 °C. This allowed the hydrocarbon vapour to condense within and fill the entire pore network of the sample. Two different hydrocarbon liquids were employed, namely either cyclohexane or cyclo-octane. Cyclohexane and cyclo-octane were chosen because their relevant molecular sizes (kinetic diameters) are just below (0.6 nm), and just above (0.8 nm), respectively, the micropore channel size in ZSM-5 zeolite. After saturation, the catalysts were placed between two susceptibility plugs within a 5 mm diameter NMR tube. A piece of tissue soaked in the hydrocarbon liquid was placed at

the top of the NMR tube to maintain the vapour pressure and reduce evaporative loss from the catalysts.

The PFG-NMR experiments were performed using a Bruker Avance 400 MHz spectrometer with static field strength of 9.4 T corresponding to a resonance frequency of 400.13 MHz for ^{1}H nuclei. PFG experiments were conducted by varying the gradient strength, g in the range of 0.674–32.030 G cm^{-1}, while keeping diffusion time, Δ, gradient length, δ, and bipolar correction delay, τ constant. Three different diffusion times, Δ, were used in this study, namely 0.015 s, 0.025 s and 0.05 s. It was generally found that the diffusivity of the slow-diffusing component (see below) was generally independent of diffusion time and so the data reported below are for a diffusion time of 0.05 s. Each experiment used 8 data points and employed 16 scans each. The observed signal attenuation was then used to calculate the apparent diffusion coefficient, D_{PFG} and tortuosity, τ_p. The log-attenuation data plots were generally curved, and thus fitted to a two diffusion component models. The curved nature of the log-attenuation plots would be consistent with little or no exchange between the two components. The slower component was attributed to the liquid within the catalyst pores. The other, much faster, component was attributed to a small amount of hydrocarbon liquid condensing at the contact points between catalyst particles. It was sometimes found that the second faster component had an apparent self-diffusivity larger than that of the bulk liquid, which would be consistent with it being located on the outside of the catalyst particles where exchange with the gas phase, and consequent diffusional enhancement, would be possible. Since the micropores will act as a relaxation sink for any molecules that spend significant time within them, it is expected that, even for cyclohexane molecules that can enter the micropores of the catalysts, the diffusion measurement will be heavily biased towards those molecules remaining within the mesopore system.

4. Results

Table 3 shows the molecular diffusivities of the slow-diffusing component, obtained in this work using PFG-NMR, for each of cyclohexane and cyclo-octane within the two different catalysts. Also shown are the platinum crystallite surface concentrations within the mesopore network obtained previously using backscattered scanning electron microscopy studies [1]. From these, two sets of data the product of the crystallite concentration and diffusivity ($C \times D$) were obtained. It can be seen that the product $C \times D$ is larger for both cyclohexane and cyclo-octane within the catalyst with the Si:Al ratio of 40. Also shown in Table 3 is the ratio of the BET-specific surface areas for solely the mesopore network within the fresh catalyst and after discharge following 48 h on-stream, as reported previously [1]. From Table 3, it can be seen that the larger value of the product $C \times D$ is associated with a larger decrease in mesopore surface area after 48 h on-stream.

Table 3
Parameters for the mesopore networks of Pt-zeolite catalysts.

	Pt H-MFI-15	Pt H-MFI-40
Crystallite concentration (C) (number of Pt particles per μm^2) [1]	0.134	0.520
Diffusivity (cyclo-octane) ($D(C8)$) × 10^{10} (m^2 s^{-1})	0.557	0.493
Tortuosity (cyclo-octane)	10.5	11.8
$C \times D(C8) \times 10^{10}$ (m^2 s^{-1} μm^{-2})	0.0746	0.256
Diffusivity (cyclohexane) ($D(C6)$) × 10^9 (m^2 s^{-1})	1.299	1.524
Tortuosity (cyclohexane)	1.278	1.089
$C \times D(C6) \times 10^9$ (m^2 s^{-1} μm^{-2})	0.174	0.792
BET area (48 h)/BET area (fresh) [1]	0.905	0.760

Table 4
Parameters for the micropore network of Pt-zeolite catalysts.

	Pt H-MFI-15	Pt H-MFI-40
Metal surface area pre-nonane (m^2 g^{-1})	0.360	0.192
Metal surface area post-nonane (m^2 g^{-1})	0.254	0.124
Metal surface area in nonane-occupied micropores (m^2 g^{-1})	0.106	0.067
Langmuir area (48 h)/Langmuir area (fresh) [1]	0.708	0.893

Table 4 shows the CO metal surface areas obtained before and after nonane pre-adsorption for the two different fresh catalysts. From these data, the metal surface area that located within the nonane-occupied microporosity was obtained by subtraction. It can be seen that the fresh Pt H-MFI-15 catalyst has a higher micropore metal surface area than the fresh Pt H-MFI-40 catalyst. Also shown in Table 4 is the ratio of the Langmuir micropore surface areas for the fresh catalyst and for a sample after discharge following 48 h on-stream, obtained in previous work [1]. It can be seen that the micropore surface area has decreased more markedly, after 48 h on-stream, for the Pt H-MFI-15 catalyst. Hence, the higher micropore metal surface area is associated with a larger drop in micropore surface area.

5. Discussion

Previous work [1] had shown that, during alkylation of benzene using ethane, the coke was deposited primarily within the microporosity of the Pt H-MFI-15 catalyst, but primarily within the mesoporosity of the Pt H-MFI-40 catalyst. As proposed above, the results obtained in this work suggest that the differing distributions of coke are controlled by the distribution of Pt metal sites and the mass transport characteristics of the mesopore network. The Pt H-MFI-15 catalyst had a lower product of mesopore diffusivity and Pt crystallite concentration than the Pt H-MFI-40 catalyst, but a higher Pt surface area in the micropores. Hence, the coking reaction was faster in the mesoporosity of the Pt H-MFI-40 catalyst, when compared with the Pt H-MFI-15 catalyst, but slower in the microporosity, consistent with the aforementioned theory. The significant influence of pore geometry of catalyst supports on coking has also been found in studies of propane dehydrogenation in Pt-ZSM-5 catalysts and others, such as Pt-beta and Pt-SBA-15 [24].

The results presented above represent the simplest form of implementation of the new technique, and the further potential of the new method is also being explored. For example, it is conceivable that the nonane within the micropores could be removed in partial stages (rather than totally at once) and both nitrogen physisorption and CO chemisorption conducted at each stage. The micropore pore size distribution obtained from nitrogen adsorption and the metal surface area obtained from chemisorption could be combined to obtain more detailed information on the spatial distribution of metal. This will be the subject of a future work. The possibility of studying other zeolite systems with different hydrocarbon pre-adsorbents is also being studied.

6. Conclusions

It has been shown that the opposite spatial distributions of coke amongst the micro- and mesoporosity within PtH-MFI catalysts with differing Si/Al ratios arose due to differing levels of metal sites within the different porosities and differences in mesopore mass transfer rates. Measurement of the spatial distribution of metal sites was facilitated by a novel nonane pre-adsorption CO chemisorptions method. It is anticipated that the nonane pre-adsorption chemisorption method can be used to investigate any other metals

that can chemisorb suitable adsorbate molecules like carbon monoxide.

Acknowledgments

The authors thank Johnson Matthey and EPSRC (under Grant No. EP/C532554) for financial support.

References

[1] L.M. Chua, T. Vazhnova, T.J. Mays, D.B. Lukyanov, S.P. Rigby, J. Catal. 271 (2010) 401.
[2] S.J. Gregg, J.F. Langford, Trans. Farad. Soc. 65 (1969) 1394.
[3] U. Ziese, K.P. de Jong, A.J. Koster, Appl. Catal. A260 (2004) 71.
[4] M. Rivallan, E. Seguin, S. Thomas, M. Lepage, N. Takagi, H. Hirata, F. Thibault-Starzyk, Angew. Chem. Int. Ed. 49 (2010) 785.
[5] R. Mann, Catal. Today 37 (1997) 331.
[6] K.-Y. Cheah, N. Chiaranussati, M.P. Hollewand, L.F. Gladden, Appl. Catal. A11 (1994) 147.
[7] S. Stapf, X.H. Ren, E. Talnishnikh, B. Blumich, Magn. Reson. Imag. 23 (2005) 383.
[8] X.-H. Ren, M. Bertmer, S. Stapf, D.E. Demco, B. Blumich, C. Kern, A. Jess, Appl. Catal. A228 (2002) 39.
[9] J. Wood, L.F. Gladden, Appl. Catal. A 249 (2003) 241.
[10] M.P. Hollewand, L.F. Gladden, Chem. Eng. Sci. 50 (1995) 309.
[11] M. Guisnet, P. Magnoux, Appl. Catal. A 212 (2001) 83.
[12] S. Lowell, J.E. Shields, M.A. Thomas, M. Thommes, Characterisation of Porous Solids and Powders: Surface Area, Pore Size and Density, Springer, Dordrecht, 2004.
[13] C. Baerlocher, Atlas of Zeolite Framework types, sixth ed., Elsevier, Oxford, 2007.
[14] F. Rouquerol, J. Rouquerol, K. Sing, Adsorption by Powders and Porous Solids, Academic Press, London, 1999.
[15] S. Roszak, K. Balasubramanian, Chem. Phys. Lett. 212 (1993) 150.
[16] S.J. Gregg, K.S.W. Sing, Adsorption, Surface Area and Porosity, Academic Press, London, 1967.
[17] B.L. Mojet, J.T. Miller, D.C. Koningsberger, J. Phys. Chem. B 103 (1999) 2724.
[18] S. Thomas, M. Rivallan, M. Lepage, N. Takagi, H. Hirata, F. Thibault Starzyk, Micropor. Mesopor. Mater. 140 (2011) 140.
[19] P. Canizares, A. de Lucas, J.L. Valverde, F. Darado, Ind. Eng. Chem. Res. 36 (1997) 4797.
[20] A.Y. Stakheev, E.S. Shipro, O. P Tkachenko, N.I. Jaeger, G. Schulz Ekloff, J. Catal. 116 (1997) 382.
[21] L.R.R. de Araujo, M. Schmal, Appl. Catal. A 235 (2002).
[22] M. Rivallan, S. Thomas, M. Lepage, N. Takagi, H. Hirata, F. Thibault Starzyk, ChemCatChem 2 (2010) 1599.
[23] M. Lepage, T. Visser, A.M.J. van der Eerden, F. Soulimani, B.M. Weckhuysen, Vib. Spectrosc. 48 (2008) 92.
[24] M.S. Kumar, A. Holmen, D. Chen, Micropor. Mesopor. Mater. 126 (2009) 152.